cortical function. It removes thioester-linked fatty acyl groups from S-acylated proteins, but is also a palmitoyl-CoA hydrolase *in vitro*[14]. Identification of the *in vivo* substrate(s) for PPT will help our understanding of the pathophysiology of INCL.

We know of only one example of lipid modifications of proteins being involved in the pathogenesis of an inherited human disease, choroideraemia, which is caused by a defect in protein prenylation[17]. It is intriguing that both choroideraemia and INCL involve defective cysteine lipid modifications, and both have choroid-retinal degeneration as prominent manifestations of disease, although the significance of these observations is unclear. Characterization of causative mutations in other representatives of NCL disorders with somewhat less dramatic symptoms than INCL will show whether they also involve defects in lipid modification of proteins. □

Received 5 May; accepted 3 July 1995.

1. Rider, J. A. & Rider, D. L. *Am. J. med. Genet.* (Suppl.) **5,** 21–26 (1988).
2. Gardiner, M. *et al. Genomics* **8,** 387–390 (1990).
3. Järvelä, I. *et al. Genomics* **9,** 170–173 (1991).
4. Williams, R. *et al. Am. J. hum. Genet.* **53,** 931–935 (1993).
5. Santavuori, P., Haltia, M. & Rapola, J. *J. dev. Med. Child Neurol.* **16,** 644–653 (1974).
6. Rapola, J. & Haltia, M. *Brain* **96,** 833–840 (1973).
7. Collins, F. *Nature Genet.* **1,** 3–7 (1992).
8. Hellsten, E. *et al. Genomics* **16,** 720–725 (1993).
9. Mäkelä, T. P. *et al. Hum. molec. Genet.* **1,** 217 (1992).
10. Hellsten, E. *et al. Genomics* **25,** 404–412 (1995).
11. Nau, M. M. *et al. Nature* **318,** 69–73 (1985).
12. Mäkelä, T. P., Saksela, K., Evan, G. & Alitalo, K. *EMBO J.* **10,** 1331–1335 (1991).
13. Perälä, M., Hänninen, M., Hästbackov, J., Elima, K. & Vuorio, E. *FEBS Lett.* **319,** 177–180 (1993).
14. Camp, L. A., Verkruyse, L. A., Afendis, S. J., Slaughter, C. A. & Hofmann, S. L. *J. biol. Chem.* **269,** 23212–23219 (1994).
15. Derewenda, Z. S. & Sharp, A. M. *Trends biochem. Sci.* **18,** 20–25 (1993).
16. Witkowski, A., Witkowska, H. E. & Smith, S. *J. biol. Chem.* **269,** 379–383 (1994).
17. Seabra, M. C., Brown, M. S. & Goldstein, J. L. *Science* **259,** 377–381 (1993).
18. Syvänen, A.-C., Sajantila, A. & Lukka, M. *Am. J. hum. Genet.* **52,** 46–59 (1993).
19. Heiskanen, M. *et al. BioTechnology* **17,** 928–929 (1994).
20. Ioannou, P. A. *et al. Nature Genet.* **6,** 84–89 (1994).
21. Syvänen, A.-C., Aalto-Setälä, K., Kontula, K. & Söderlund, H. *FEBS Lett.* **258,** 71–74 (1989).
22. Camp, L. A. & Hofmann, S. L. *J. biol. Chem.* **268,** 22566–22574 (1993).
23. Erlanson, C. *Scand. J. Gastroenter.* **5,** 333–336 (1970).
24. Stacey, A. & Schnieke, A. *Nucleic Acids Res.* **18,** 2829 (1990).
25. Taylor, J. W., Ott, J. & Eckstein, F. *Nucleic Acids Res.* **13,** 8764–8765 (1985).
26. Sanger, F., Nicklen, S. & Coulson, A. R. *Proc. natn. Acad. Sci. U.S.A.* **74,** 5463–5467 (1977).
27. Felgner, P. L. *et al. Proc. natn. Acad. Sci. U.S.A.* **84,** 7413–7417 (1987).
28. Proia, R. L., D'azzo, A. & Neufeld, E. F. *J. biol. Chem.* **259,** 3350–3354 (1984).
29. Laemmli, U. K. *Nature* **227,** 680–685 (1970).
30. Riikonen, A. *et al. DNA Cell Biol.* **13,** 257–264 (1994).

ACKNOWLEDGEMENTS. J.V. and E.H. contributed equally to this work. We thank A. Jalanko, A.-C. Syvanen and A. Suomalainen for comments; T. Airaksinen, J. Schriner, B. Doerrler and S. Madden for technical assistance; M. Heiskanen for help in FiberFISH analysis. This work was supported by the Rinnekoti Research Foundation, the Paulo Foundation, the Academy of Finland, the 350th Anniversary Foundation of the University of Helsinki, the NIH and the Medical Scientist Training Program.

Brain regions associated with retrieval of structurally coherent visual information

Daniel L. Schacter*, Eric Reiman†‡, Anne Uecker§, Michael R. Polster‖, Lang Sheng Yun‡¶ & Lynn A. Cooper#

* Department of Psychology, Harvard University, 33 Kirkland Street, Cambridge, Massachusetts 02138, USA
† Department of Psychiatry, University of Arizona, Tucson, Arizona 85721, USA
‡ Positron Emission Tomography Center, Good Samaritan Regional Medical Center, Phoenix, Arizona 85006, USA
§ Division of Neural Systems, Memory and Aging, University of Arizona, Tucson, Arizona 85721, USA
‖ Department of Psychology, University of Victoria at Wellington, Wellington, New Zealand
¶ Department of Computer Science and Engineering, Arizona State University, Tempe, Arizona 85287, USA
# Department of Psychology, Columbia University, New York, New York 10027, USA

An object's global, three-dimensional structure may be represented by a specialized brain system involving regions of inferior temporal cortex[1–3]. This system's role in object representation can be understood by experiments in which people study drawings of novel objects with possible or impossible three-dimensional structures, and later make either possible/impossible object decisions or old/new recognition decisions about briefly flashed studied and non-studied objects. Although object decisions about possible objects are facilitated by prior study, there is no corresponding facilitation for impossible objects, thereby implicating a system that is specifically involved in the representation of structurally coherent visual objects[4]. Here we show, by positron emission tomography (PET), that increases in blood flow in inferior temporal regions are associated with object decisions about possible but not impossible objects, and that there are increases in the vicinity of the hippocampal formation associated with episodic recognition of possible objects.

Ten 31-slice PET images of regional cerebral blood flow in 16 healthy females were obtained using the ECAT 951/31 scanner (Siemens, Knoxville, Tennessee), 45 mCi intravenous bolus injections of $H_2{}^{15}O$, and 60-s scans as they viewed 50-ms presentations of individual possible or impossible objects. During the first two scans, subjects pressed a button with their index finger when an object disappeared from the screen, providing no-decision baseline images that controlled for visual stimulation and movement. Subjects then studied a series of 20 possible and 20 impossible objects in the absence of a scan. During the next four scans, subjects made decisions about whether the objects were possible or impossible during four separate blocks of 20 old possible, 20 new possible, 20 old impossible, and 20 new impossible objects. The final four scans used the same arrangement of blocks, but subjects made old/new recognition memory decisions (Fig. 1). Despite procedural modifications necessitated by the demands of PET, behavioural data concerning object decision and recognition performance are in close agreement with previous results (Table 1). For each subtraction described below, automated algorithms were used to align the 10 PET images from each subject, spatially transform them into the coordinates of a standard brain atlas, control for variations in whole brain measurements, compute normalized *t*-score maps of significant increases in regional blood flow (maximal *t*-score > 2.58, $P < 0.005$, uncorrected for multiple comparisons), and superimpose the maps onto the subjects' spatially transformed and averaged magnetic resonance images[5–8].

To examine blood flow increases associated with object decisions about old and new, structurally coherent and structurally incoherent objects, the no-decision baseline scan was subtracted from the new and old object decision scans for possible and impossible objects, respectively. Object decisions about possible objects were associated with significant blood flow increases in the inferior temporal gyrus and the adjacent fusiform (occipito-temporal) gyrus (Fig. 2), bilaterally for old objects and on the right for new objects. In contrast, object decisions about old and new impossible objects were not associated with significant blood flow increases in the inferior temporal or fusiform gyri; the only exception was a trend ($P < 0.05$) in the right inferior temporal region in the new-object decision condition. To examine blood flow increases associated with changes in object decisions about structurally coherent objects as a result of studying them during the tool/support encoding task (priming effects; see Fig. 1, Table 1), the new possible-object decision scan was subtracted from

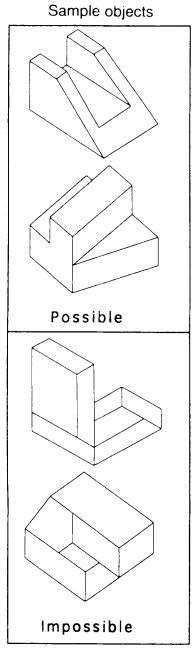

Experimental Design

Task	Scan	Objects	Condition
Keypress To offset object	1 2	Possible and impossible	No-decision baseline
Tool-support judgement	- - -	Possible and impossible	Encoding task
Object decision Possible or impossible structure	3 4 5 6	New possible New impossible Old possible Old impossible	New OD New OD Old OD Old OD
Recognition Previously studied or new object	7 8 9 10	New possible New impossible Old possible Old impossible	New RN New RN Old RN Old RN

FIG. 1 Examples of objects used in the experiment are shown on the left. Possible objects are structures that could exist in the three-dimensional world. Impossible objects contain local edge or surface violations and hence could not be constructed as connected, three-dimensional solids. The overall experimental design is displayed on the right. Ten separate scans were used, each involving computerized presentation of 20 consecutive objects according to the following sequence: (1) a cross-hair fixation point for 250 ms; (2) a blank interval of 100 ms; (3) an object at central fixation for 50 ms followed by a key-press response; and (4) an inter-trial delay of 2,500 ms. The no-decision baseline scans (1 and 2) served as a control for visual exposure to the objects and actuation of a key-press response. Subjects next engaged in an encoding or study task, during which no scanning occurred. They saw 40 objects (20 possible and 20 impossible), presented individually in a random sequence, for 5 s each. Subjects indicated whether each object would best be used as a tool or for support. Previous research has shown that the tool/support judgement is one of several encoding tasks that produce significant effects of study, known as priming effects, on the object decision task[29]. Object decisions (OD) were assessed in the next four scans. During two of these scans (3 and 4; new possible and new impossible), subjects made decisions of possible/impossible about objects that had not appeared previously at any point in the experiment; during the other two scans (5 and 6; old possible and old impossible), they made the same decisions about objects that had appeared during the encoding task. Finally, episodic recognition (RN) was assessed by using a similar arrangement of four scans, except that subjects indicated whether or not they remembered seeing an object during the encoding task. The new possible and new impossible scans (7 and 8) each used objects that had not appeared previously in any phase of the experiment, whereas the old possible and old impossible scans (9 and 10) used objects that had appeared during the encoding task and during scans 5 or 6 of the object decision task. Assignment of objects to conditions and order of scans within conditions was completely counterbalanced for 12 subjects and partly counterbalanced for 4 subjects.

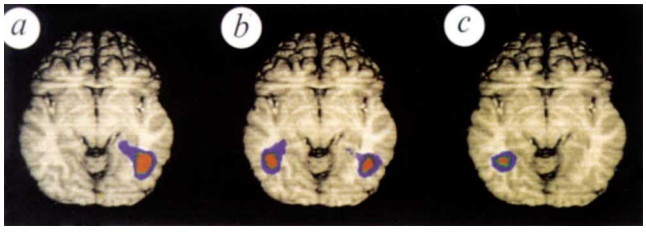

FIG. 2 For possible visual objects: *a*, new-object decision minus no-decision baseline; *b*, old-object decision minus no-decision baseline; and *c*, old-object decision minus new-object decision subtractions revealed significant blood flow increases in the vicinity of right, bilateral, and left inferior temporal and fusiform gyri, respectively. For each subtraction, automated algorithms were used to characterize significant increases in regional blood flow (those with a maximal normalized *t*-value > 2.58, $P < 0.005$, uncorrected for multiple comparisons[6–8]). For *a*–*c*, normalized *t*-value maps were superimposed onto a magnetic resonance image which was transformed into the coordinates of a brain atlas[5,7], volume rendered, and resected posterior to a coronal plane through the anterior commissure to reveal inferior temporal blood flow increases in a horizontal section 8 mm inferior to a plane through the anterior and posterior commissures. Increases in inferior temporal blood flow are shown in red, green and blue, which correspond to normalized *t*-values greater than 2.58, 2.33 and 1.64, and uncorrected probabilities less than 0.005, 0.01 and 0.05, respectively. Atlas coordinates and *t*-values of these and other significant blood flow increases are available from the author on request.

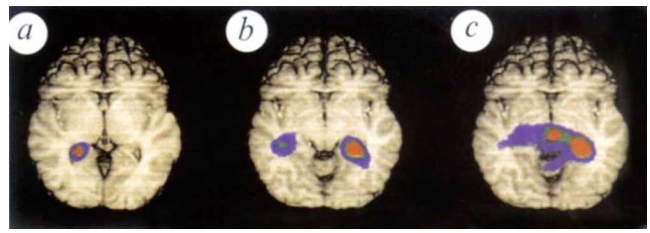

FIG. 3 For possible visual objects: *a*, new-recognition memory minus no-decision baseline; *b*, old-recognition memory minus no-decision baseline; and *c*, old-recognition memory minus new-recognition memory subtractions revealed significant blood flow increases in the vicinity of the left, bilateral and right hippocampus, respectively. For each subtraction, automated algorithms were used to characterize significant increases in regional blood flow (those with a maximal normalized *t*-value > 2.58, $P < 0.005$, uncorrected for multiple comparisons[6–8]). For *a*–*c*, normalized *t*-value maps were superimposed onto a magnetic resonance image which was transformed into the coordinates of a brain atlas[5,7], volume rendered, and resected posterior to a coronal plane through the anterior commissure to reveal hippocampal blood flow increases in a horizontal section 8 mm inferior to this plane in *b* and *c*. Increases in hippocampal blood flow (and additional increases in the vicinity of the parahippocampal gyrus and midbrain in *b*) are shown in red, green and blue, which correspond to normalized *t*-values greater than 2.58, 2.33 and 1.64, and uncorrected probabilities less than 0.005, 0.01 and 0.05, respectively. Atlas coordinates and *t*-values of these and other significant blood flow increases are available from the author on request.

the old possible-object decision scan. This comparison revealed significant blood flow increases in the left inferior temporal/fusiform region (Fig. 2). When the same subtraction was performed for impossible objects, there were no significant blood flow increases in the inferior temporal and fusiform gyri. Although these findings suggest an association between priming of possible objects and left inferior temporal/fusiform blood flow increases, they could also be due to more possible but not more impossible objects being perceived as structurally coherent in the old-object decision condition than in the new-object decision condition.

Post hoc analyses were performed to characterize more directly those blood flow increases that were preferentially related to possible versus impossible objects, and those that were preferentially related to the left versus right hemisphere. Right inferior temporal and fusiform blood flow increases during object decision for possible objects were greater than those in the left hemisphere ($P<0.005$), and were also greater than those in the right hemisphere during object decision for impossible objects ($P<0.05$). Left inferior temporal and fusiform blood flow increases associated with studying possible objects were greater than those in the right hemisphere ($P<0.005$), and were also greater than those in the left hemisphere during the same comparison for impossible objects ($P<0.05$).

These findings are consistent with our proposal that a system involving inferior temporal regions is involved in the representation of a visual object's global, three-dimensional structure. Studies with non-human primates implicate inferior temporal regions in computing size-invariant representations of global object structure[1,3,9], and studies with human volunteers show that effects of prior study on object decisions about possible objects are size invariant[10] and depend on encoding of global object structure[4]. Several kinds of evidence implicate the fusiform gyri in high-level object recognition[11,12] and global or holistic visual representation[13–15].

For impossible objects only, both the old-object decision and new-object decision minus no-decision baseline comparisons revealed significant blood flow increases in the vicinity of the left hippocampal formation and the pulvinar bilaterally. The hippocampal formation has been linked previously with encoding of novel or unexpected stimuli[16–19] and the pulvinar has been implicated in controlling attention to visually salient stimuli[20]. Accordingly, these increases could reflect encoding of the novel or unusual features of impossible objects.

To examine blood flow increases associated with the recognition task, each no-decision baseline (possible or impossible) was subtracted from the corresponding old or new recognition scan, respectively (Fig. 3). For both possible and impossible objects, the new recognition minus no-decision baseline comparison revealed significant blood flow increases in the vicinity of the hippocampal formation bilaterally, predominantly on the left. The old-recognition minus baseline comparisons also revealed significant blood flow increases in the vicinity of the hippocampal formation, bilaterally for possible objects and predominantly on the left for impossible objects. For impossible objects only, these comparisons again revealed significant blood flow increases in the vicinity of the pulvinar bilaterally. Post hoc comparisons indicate that blood flow increases in the left hippocampal formation during the new-object decision, old-object decision, new recognition, and old recognition minus no-decision baseline comparisons for impossible objects were greater than those in the right ($P<0.05$), and were also greater than those in the left during the same comparisons for possible objects ($P<0.05$).

To examine blood flow changes specifically associated with memory for the appearance of an object in the study list, here referred to as episodic memory, the new-recognition condition was subtracted from the old-recognition condition (Fig. 3). For possible objects, this comparison revealed blood flow increases in the vicinity of the right hippocampal formation, left parahippocampal and fusiform gyri, the midbrain, and left dorsolateral prefrontal cortex (Brodmann areas 10, 44–46). For impossible objects, for which there was less accurate episodic memory (Table 1), the same comparisons revealed no significant blood flow increases. Post hoc comparisons indicate that the right hippocampal/parahippocampal blood flow increases during episodic memory for possible objects were greater than those in the left ($P<0.05$), and were greater than those in the right during the same comparisons for impossible objects ($P<0.05$).

Our results are consistent with evidence supporting involvement of the hippocampal formation[21–24] and dorsolateral prefrontal cortex[24–27] in episodic memory. Failure to detect significant blood flow increases in association with episodic recognition of impossible objects could indicate that recognition of these objects was not sufficiently robust, that the right hippocampal region is less involved in recognition of impossible than of possible objects, or that right hippocampal activation depends on both episodic memory and other factors that are not yet well understood[27].

This study and others have activated the hippocampal formation, but several previous memory experiments failed to do so[25–27]. Although the exact reasons for the contrasting results remain elusive[27,28], we suspect that the novelty of our objects is relevant. We suggest that the left hippocampal/parahippocampal region participated in some aspect of response to these novel stimuli (such as object encoding or identification of a mismatch between internal expectations and novel stimuli), whereas the right hippocampal/parahippocampal region was involved in episodic retrieval of the objects.

Our study attempted to indicate brain regions that are specifically involved in object decision and recognition tasks that we have previously studied behaviourally, so we presented possible or impossible objects in all conditions. It is unknown whether

TABLE 1 Object decision and recognition performance

Task	Possible objects Old	Possible objects New	Impossible objects Old	Impossible objects New
Object decision	0.67	0.56	0.63	0.58
Old/new recognition	0.82	0.33	0.68	0.36

For the object decision test, the table entries refer to the proportion of correct object decisions for old objects, which appeared previously during the encoding task, and the proportion of correct object decisions for new objects, which had not appeared during the encoding task. For possible objects, subjects made more correct decisions about studied than non-studied objects ($t(15)=3.01$, $P<0.005$), whereas, for impossible objects, significant differences between studied and non-studied objects were not observed ($t(15)<1$). Nearly identical results were obtained in a purely behavioural pilot study using identical test procedures, carried out before the PET study. These findings replicate previously published results from a variety of conditions in numerous experiments[2,4,10,29]. Overall levels of object decision accuracy for new and old objects are also closely comparable to data from previously published behavioural studies. For the yes/no recognition test, the table entries refer to the proportion of 'old' responses made to old objects (the hit rate) and the proportion of 'old' responses to new objects (the false-alarm rate). To compare recognition accuracy for possible and impossible objects, we computed a corrected recognition score by subtracting the false-alarm rate from the hit rate. The corrected recognition score for possible objects (0.49) was significantly higher than the corrected recognition score for impossible objects (0.32), ($t(15)=4.58$, $P<0.001$). Nearly identical results were obtained in the pilot study using a separate set of subjects and the same test procedures. These findings replicate results from numerous previously published experiments[2,4,10,29]. The overall levels of 'old' and 'new' responses are also similar to published results from the same experiments. That we replicated both the quantitative and qualitative findings of previous research is important because the demands of PET scanning required that we present old possible, new possible, old impossible, and new impossible objects in separate blocks. This is a substantial departure from the standard practice of intermixing objects from different conditions, but our behavioural data indicate that task performance is indistinguishable from performance under standard experimental conditions.

simply looking at possible or impossible objects, as opposed to a condition in which non-object stimuli are presented, produces differential blood flow increases for possible and impossible objects. A study using additional controls is necessary to determine how the blood flow changes reported here are related to those involved in passive perception of possible and impossible objects.

Additional significant blood flow changes will be described in a subsequent report. For instance, for both possible and impossible objects, the new-object decision, old-object decision, new recognition and old recognition minus no-decision baseline comparisons all revealed increases in the vicinity of dorsolateral prefrontal cortex (Brodmann areas 10, 44–46), which could be involved in the executive operations associated with making a decision.

Our study provides direct neuroanatomical evidence from the normal human brain that inferior temporal and fusiform gyri are selectively involved in computing global representations of structurally coherent three-dimensional objects, and extends our knowledge of the neural systems involved in episodic memory for visual objects. □

Received 28 October 1994; accepted 28 June 1995.

1. Miyashita, Y. *A. Rev. Neurosci.* **16,** 245–269 (1993).
2. Schacter, D. L., Cooper, L. A., Tharan, M. & Rubens, A. B. *J. cogn. Neurosci.* **3,** 118–131 (1991).
3. Tanaka, K. *Science* **262,** 685–688 (1993).
4. Schacter, D. L., Cooper, L. A. & Delaney, S. M. *J. exp. Psychol.* **119,** 5–24 (1990).
5. Collins, D. L., Neelin, P., Peters, T. M. & Evans, A. C. *J. comput. assist. Tomogr.* **18,** 192–204 (1994).
6. Friston, K. J. *et al. J. cerebr. Blood Flow Metab.* **10,** 458–466 (1991).
7. Talairach, J. & Tournoux, P. *Co-planar Stereotaxic Atlas of the Human Brain* (Thieme Medical, New York, 1988).
8. Mintun, M. A. & Lee, K. S. *J. nucl. Med.* **31,** 816 (1991).
9. Gross, C. G. *Phil. Trans. R. Soc.* B**335,** 245–246 (1992).
10. Cooper, L. A., Schacter, D. L., Ballesteros, S. & Moore, C. *J. exp. Psychol., Learn. Mem. Cogn.* **18,** 43–57 (1992).
11. Kosslyn, S. M. *et al. Brain* (in the press).
12. Sergent, J., Ohta, S. & MacDonald, B. *Brain* **115,** 15–36 (1992).
13. Allison, T. *et al. J. Neurophysiol.* **71,** 821–825 (1994).
14. Damasio, A. R., Damasio, H. & VanHoesen, G. W. *Neurology* **32,** 331–341 (1982).
15. Haxby, J. V. *et al. J. Neurosci.* **14,** 6336–6353 (1994).
16. Gray, J. A. *The Neuropsychology of Anxiety* (Oxford Univ. Press, 1982).
17. Stern, C. *et al. Soc. Neurosci. Abstr.* **20,** 530 (1994).
18. Tulving, E. *et al. NeuroReport* **5,** 2525–2528 (1994).
19. Vinograda, O. S. *The Hippocampus* Vol. 2 (eds Isaacson, R. L. & Pribram, K. H.) (Plenum, New York, 1978).
20. Robinson, D. L. & Petersen, S. E. *Trends Neurosci.* **15,** 127–132 (1992).
21. Frackowiak, R. S. J. *Trends Neurosci.* **17,** 109–115 (1994).
22. Grasby, P. M. *et al. Neurosci. Lett.* **163,** 185–188 (1993).
23. Jones-Gotman, M. *et al. Soc. Neurosci. Abstr.* **19,** 1002 (1993).
24. Squire, L. R. *et al. Proc. natn. Acad. Sci. U.S.A.* **89,** 1837–1841 (1992).
25. Shallice, T. *et al. Nature* **368,** 633–635 (1994).
26. Tulving, E. *et al. Proc. natn. Acad. Sci. U.S.A.* **91,** 2012–2015 (1994).
27. Buckner, R. *et al. J. Neurosci.* **15,** 12–29 (1995).
28. Buckner, R. & Tulving, E. *Handbook of Neuropsychology* (eds Boller, F. & Grafman, J.) 439–466 (Elsevier, Amsterdam, 1995).
29. Schacter, D. L. & Cooper, L. A. *J. exp. Psychol., Learn. Mem. Cogn.* **19,** 995–1009 (1993).

ACKNOWLEDGEMENTS. We thank D. Bandy, N. Blocher, A. Evans, M. Mintun, K. Nelson and K. Zemanick for their assistance. This work was supported by grants from the McDonnell-Pew Program in Cognitive Neuroscience, the Robert S. Flinn Foundation, and the NIMH.

Inhibition by anandamide of gap junctions and intercellular calcium signalling in striatal astrocytes

Laurent Venance*, Daniele Piomelli†, Jacques Glowinski* & Christian Giaume*‡

* INSERM U114, Collège de France, 11 Place Marcelin Berthelot, 75231 Paris Cedex 05, France
† The Neurosciences Institute, 3377 North Torrey Pines Court, La Jolla, California 90237, USA

ANANDAMIDE, an endogenous arachidonic acid derivative that is released from neurons and activates cannabinoid receptors[1], may act as a transcellular cannabimimetic messenger in the central nervous system[2–4]. The biological actions of anandamide and the identity of its target cells are, however, still poorly documented[5]. Here we show that anandamide is a potent inhibitor of gap-junction conductance and dye permeability in striatal astrocytes. This inhibitory effect is specific for anandamide as compared to co-released congeners[4] or structural analogues, is sensitive to pertussis toxin and to protein-alkylating agents, and is neither mimicked by cannabinoid-receptor agonists nor prevented by a cannabinoid-receptor antagonist. Glutamate released from neurons evokes calcium waves in astrocytes[6] that propagate via gap junctions[7–9], and may, in turn, activate neurons distant from their initiation sites in astrocytes[10–12]. We find that anandamide blocks the propagation of astrocyte calcium waves generated by either mechanical stimulation or local glutamate application. Thus, by regulating gap-junction permeability, anandamide may control intercellular communication in astrocytes and therefore neuron–glial interactions.

The conductance of gap junctions (GJ) was monitored in pairs of cultured striatal astrocytes from embryonic mice by using the double whole-cell recording (DWCR) method[13] (Fig. 1*Aa*, *b*). The junctional conductance, which was 14.4 ± 2.7 nS (mean ± s.e.m.; $n = 26$) in the control, was reduced to 1.1 ± 1.2 nS ($n = 14$, in which 8 pairs were completely uncoupled) by 5 μM anandamide, but not by the cannabinoid agonist CP55940 (1 μM) (20.5 ± 5.3 nS; $n = 6$) (Fig. 1*B*). This inhibitory effect of anandamide on GJ permeability was confirmed by using the scrape-loading dye-transfer technique[14]. The intercellular diffusion of Lucifer yellow was significantly decreased and even greatly inhibited when the cells were incubated for 10 min with anandamide (1 μM and 5 μM, respectively) (Fig. 1*Ca–c*, *D*). The inhibition evoked by anandamide (5 μM) was reversible, and comparable to that evoked by the uncoupling agent 18α-glycyrrhetinic acid[15] (10 μM) (Fig. 1*D*), being already apparent after 2 min exposure (data not shown).

In contrast to anandamide, two synthetic cannabinoid-receptor agonists, Win-55212-2 (5 μM) and CP55940 (1 μM), had no effect on GJ permeability (Fig. 1*D*), although at the same concentrations these two compounds, as anandamide, inhibited the isoprenaline(1 μM)-induced production of cyclic AMP in striatal astrocytes (S. Sagan, unpublished results). Moreover, the antagonist at CB1-type cannabinoid receptors[16], SR141716A (0.5 μM; 10 min pretreatment), did not reduce the anandamide response (Fig. 1*D*). Therefore, anandamide seems to modulate GJ permeability in striatal astrocytes through a mechanism distinct from central cannabinoid-receptor activation. When cells were pretreated in the presence of the phosphodiesterase inhibitor IBMX (1 mM) with agents known to increase cAMP concentration (such as isoprenaline or forskolin, at 10 μM for 10 min), the effectiveness of anandamide on GJ permeability was not altered, suggesting that a reduction of cAMP level is not involved in this process. In addition, neither the protein-kinase inhibitors H7(0.1 mM, 30 min) or staurosporine (1 μM, 30 min), which have a large range of action, nor the phosphatase inhibitor okadaic acid (0.1 μM, 40 min) prevented GJ uncoupling induced by anandamide (5 μM, 10 min).

The chemical structure of anandamide (*N*-arachidonoyl ethanolamine) includes the polyunsaturated fatty acyl moiety of arachidonic acid (AA), which inhibits GJ permeability in astrocytes[17]. However, several observations suggested that anandamide does not act directly on striatal astrocyte GJ by mimicking the uncoupling effect of exogenous application of AA. First, anandamide was ~10 times more potent than AA in uncoupling striatal astrocytes (Fig. 1*D*). Second, pertussis toxin

‡ To whom correspondence should be addressed.